[9] Recent examples of singlet-oxygen oxidation of furans can be found in dysidiolide syntheses: a) E. J. Corey, B. E. Roberts, *J. Am. Chem. Soc.* **1997**, *119*, 12425; b) S. R. Magnuson, L. Sepp-Lorenzino, N. Rosen, S. J. Danishefsky, *J. Am. Chem. Soc.* **1998**, *120*, 1615.

[10] The authors thank Dr. T. Kaneko and Dr. T. T. Dabrah of the Pfizer Central Research for providing a trace sample of natural CP-225,917 and several small samples of CP-263,114 from separate fermentation processes.

[11] Use of trimethylsilyldiazomethane leads to a trimethyl ester as the product from a ring opening of the anhydride. Some diazomethane methylations required 2-pentene as cosolvent to prevent side reactions at the two side-chain olefins.

[12] **9**: IR(film): $\tilde{\nu}=2921$, 1798, 1767, 1736 cm^{-1}; ^1H NMR ($CDCl_3$, 500 MHz): $\delta=5.81$(s, 1H), 5.45–5.39 (m, 4H), 4.21 (dd, $J=12.2$, 3.0 Hz, 1H), 3.71 (s, 3H), 3.29 (s, 1H), 3.25 (d, $J=17.5$ Hz, 1H), 3.08 (d, $J=8.3$ Hz, 1H), 2.95 (d, $J=17.5$ Hz, 1H), 2.64 (dd, $J=19.2$, 2.2 Hz, 1H), 2.29–2.20 (m, 3H), 2.04–2.00 (m, 3H), 1.94–1.89 (m, 3H), 1.64–1.62 (m, 6H), 1.25–1.14 (m); HR-MS (FAB) calcd for $C_{32}H_{38}O_9Na$ $[M+Na]^+$: 589.2413, found: 589.2391.

[13] **10**: IR(film): $\tilde{\nu}=2927$, 1792, 1768, 1740 cm^{-1}; ^1H NMR ($CDCl_3$, 500 MHz): $\delta=5.66$ (d, $J=1.9$ Hz, 1H), 5.50–5.30 (m, 4H), 4.54 (t, $J=8.1$ Hz, 1H), 3.73 (s, 3H), 3.53 (s, 1H), 3.25 (d, $J=17.4$ Hz, 1H), 3.08 (d, $J=19.5$ Hz, 1H), 2.93 (d, $J=17.4$ Hz, 1H), 2.74–2.69 (m, 3H), 2.53 (m, 1H), 2.35–2.25 (m, 4H), 2.12 (dd, $J=13.6$, 8.8 Hz, 1H), 1.94–1.91 (m, 2H), 1.64–1.62 (m, 6H), 1.25–1.14 (m); HR-MS (FAB) calcd for $C_{32}H_{38}O_9Na$ $[M+Na]^+$: 589.2413, found: 589.2415.

[14] The trace fermentation acid samples came from several different sources which differed in the amount of the 7*S* system **17** (and subsequently its methyl ester **11**). The ratio of **2**:**17** did not change following storage of the samples in our premises for five months at $-78\,^{\circ}C$.

[15] Separation conditions of **1**, **2**, **15**, and **17:** Reversed-phase HPLC column: Metachem Inertsil 5 μ ODS2, 0.002 % H_3PO_4:CH_3CN = 4:6. Retention time: **15** (16 min), **1** (17 min), **2** (32 min), **17** (34 min). It is also crucial to inject the sample in a 1/1 mixture of 0.1 % H_3PO_4 in CH_3CN. We note also that the chromatography per se does not effect the homogeneity of the samples. Hence, we are confident that the 7*S* isomer we detected was present in the original samples.

[16] Another pathway not invoking enediol **12** would involve a reversible C6-C7 α-ketol shift with an intervening rotation about the C6-C7 σ bond. This step would effectively epimerize C7 without the necessary scrambling of the ketol. For this "ketol-shift" pathway, as well as the enediol pathway, to be viable, it would be crucial that the 7-hydroxy-6-ketone be much more stable than the 6-hydroxy-7-ketone isomers in both the 7*R* and 7*S* series.

[17] Dess–Martin periodinane: a) D. B. Dess, J. C. Martin, *J. Org. Chem.* **1983**, *48*, 4155; b) D. B. Dess, J. C. Martin, *J. Am. Chem. Soc.* **1991**, *113*, 7277; c) S. D. Meyer, S. L. Schreiber, *J. Org. Chem.* **1994**, *59*, 7549; d) R. E. Ireland, L. Liu, *J. Org. Chem.* **1993**, *58*, 2899; review of TPAP/NMO oxidation: S. V. Ley, J. Norman, W. P. Griffith, S. P. Marsden, *Synthesis* **1994**, 639.

Electron Microscopy Reveals the Nucleation Mechanism of Zeolite Y from Precursor Colloids**

Svetlana Mintova, Norman H. Olson, and Thomas Bein*

Zeolites are crystalline, porous solids whose intricate pore and channel systems in the molecular size range of 0.3 to about 1.5 nm are the basis for their immense importance in catalysis, separations, and ion exchange.[1–4] Although numerous studies have addressed the preparation of zeolites, it has been very difficult to model the complex mechanism by which they assemble from framework constituent precursor species under hydrothermal synthesis conditions.

An improved understanding of the synthesis mechanism is pivotal for the design of new zeolites (only about 100 structures are known so far), and for the preparation of novel zeolitic assemblies such as zeolite thin films for membrane reactors, monoliths, or functional nanostructures.[5] Here we report direct, high-resolution electron microscopic evidence for the nucleation mechanism of zeolite Y (faujasite structure type; FAU) in nanoscale amorphous aluminosilicate gel particles, followed by full conversion of the gel aggregates into 25–35 nm large single crystals of zeolite Y. Further crystallization of the colloidal zeolite Y suspension is mediated by soluble aluminosilicate species.

Different mechanisms have been discussed regarding nucleation and crystallization of zeolites, based on experimental evidence obtained with various methods such as X-ray diffraction and scattering, solid-state NMR spectroscopy, atomic force microscopy, and electron microscopy.[6–22] These include transformation of the precursor gel phase, aggregation and realignment of preassembled building blocks containing template molecule/(alumino)silicate clusters, and assembly of soluble small species from solution. Most of the above techniques give information about the final crystalline product; however, imaging the initial stage of zeolite formation has not previously been possible.

Several molecular sieves, including zeolite A, Y, L, ZSM-5, silicalite-1, TS-1, and $AlPO_4$-5 can be made in colloidal form with particle sizes in the nanometer range.[23–28] Recently, we reported a detailed study of the very early stages of zeolite A

[*] Prof. T. Bein, Prof. S. Mintova[+]
Department of Chemistry, Purdue University
West Lafayette, IN 47907 (USA)
New Address:
Institut für Physikalische Chemie der Universität
D-81377 München (Germany)
Fax: (+49) 89-2180-7624
E-mail: tbein@cup.uni-muenchen.de
Dr. N. H. Olson
Department of Biology, Purdue University
West Lafayette, IN 47907 (USA)
[+] On leave from:
Central Laboratory of Mineralogy and Crystallography
Bulgarian Academy of Science, 92 Rakovski Street
1000 Sofia (Bulgaria)

[**] This research was supported by the US National Science Foundation (T.B. and S.M.) and through an NIH biology grant (N.H.O.).

  1433-7851/99/3821-3201 $ 17.50+.50/0

crystal growth at room temperature, where amorphous gel particles were converted into nanoscale single crystals.[28]

Zeolite Y can be viewed as the archetype zeolite owing to its enormous importance in catalysis (hydrocracking of petroleum) and its large stable pore structure, which makes it an ideal host for novel nanocomposites.[1] In this study we examined the entire process of gel formation, nucleation, and crystal growth of this important zeolite at 100 °C in a colloidal model system. The structural evolution of these species was followed at different time intervals with high-resolution transmission electron microscopy (HR-TEM) at reduced dose in the field-emission mode. To compliment the HR-TEM studies, X-ray diffraction, dynamic light scattering (DLS), thermogravimetric analysis (TGA), and IR spectroscopy were used to monitor the crystallization process.

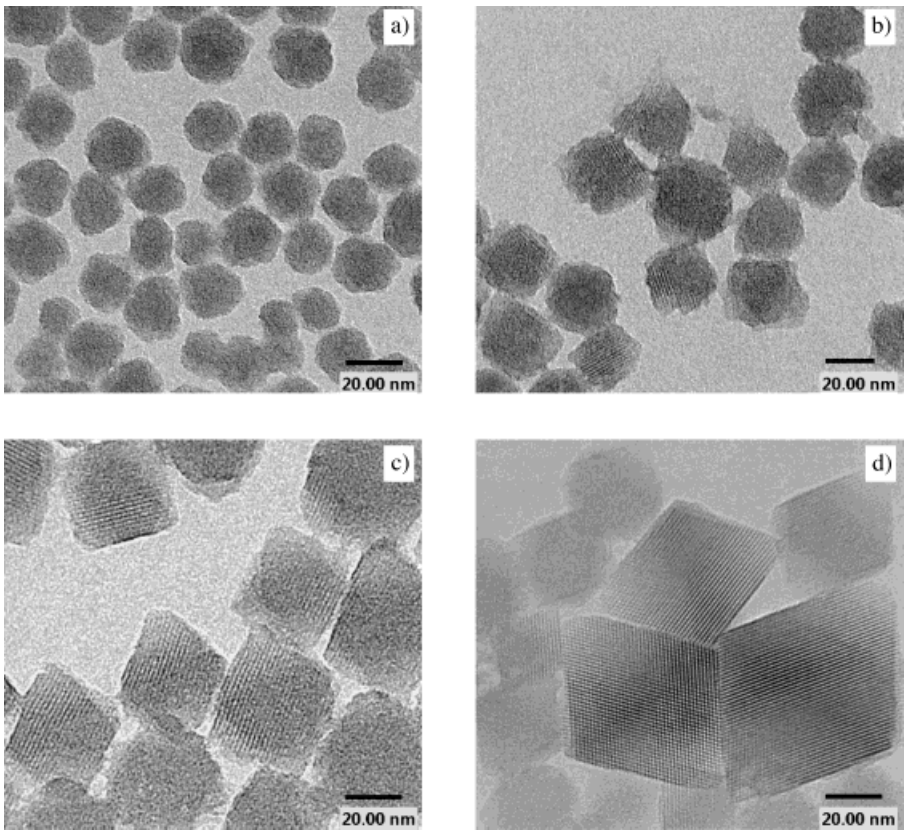

Figure 2. Particles in a) freshly prepared aluminosilicate solution for the synthesis of zeolite Y and after hydrothermal treatment at 100 °C for b) 28, c) 48, and d) 75 h.

The aggregates in the freshly prepared colloidal solution at room temperature are shown to be amorphous by X-ray diffraction (Figure 1 a). The TEM image reveals the presence of 25–35 nm large amorphous gel particles having sharp edges (Figure 2 a). These gel particles are the precursors for the nucleation stage of the FAU crystals. The start of crystallization of zeolite Y from this colloidal solution requires heating at 100 °C in excess of 24 h—representing the well-known "induction period" in zeolite synthesis. After 24 h at 100 °C, the XRD pattern shows that the resulting aluminosilicate consists of amorphous material only (Figure 1 b). The TEM image of this sample is similar to that for the freshly prepared synthesis mixture. A complementary IR study was performed of both freshly prepared solutions and samples heated for 24 h (Figure 3 a, b). The IR spectra contain only a band at 470 cm^{-1}, which is assigned to structure-insensitive T–O bending modes of tetrahedral TO_4 units (T = Si or Al), and confirm the amorphous nature of the above sample.

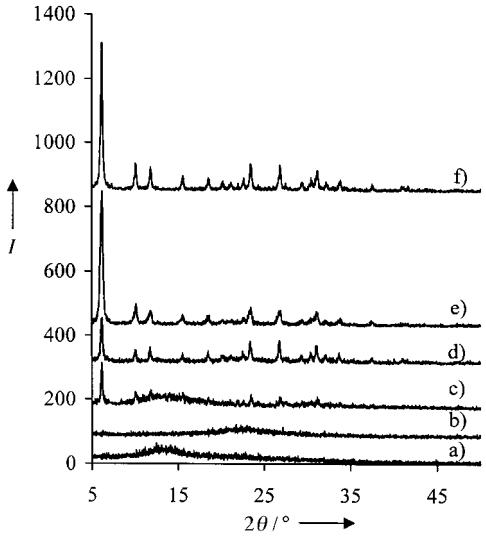

Figure 1. Powder diffraction patterns of a) the freshly prepared solution for the synthesis of zeolite Y (containing all reagents) and after hydrothermal treatment for b) 24, c) 28, d) 38, e) 55, and f) 75 h.

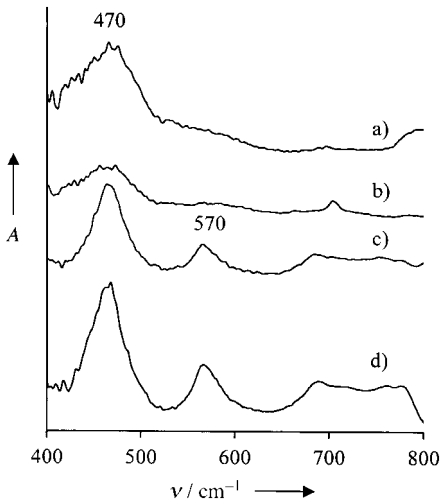

Figure 3. IR spectra of a) the freshly prepared solution for the synthesis of zeolite Y and after hydrothermal treatment for b) 24, c) 28, and d) 55 h. Samples were isolated by centrifugation and prepared as KBr pellets.

  1433-7851/99/3821-3202 $ 17.50+.50/0

Crystalline zeolite Y emerged after 28 h of hydrothermal treatment of the initial solution, and diffraction lines began to appear (Figure 1c). The HR-TEM images of this sample show crystalline nanoparticles of approximately 10 to 20 nm in size (Figure 2b). The linear size of these crystals corresponds to only 7, 9, and 15 unit cells (Figure 4). These particles show a

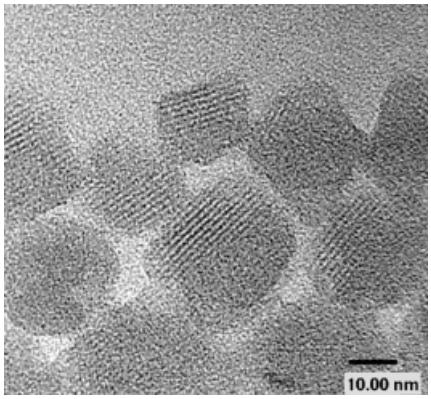

Figure 4. HR-TEM image of FAU crystals grown in the amorphous gel aggregates after hydrothermal treatment for 28 h at 100 °C.

lattice spacing of 14 Å attributed to the (111) planes of the FAU structure.[29] Strikingly, the crystals always nucleate on the periphery of the amorphous gel aggregates (Figure 4). Our observations provide strong evidence for one of the nucleation mechanisms of zeolite X (FAU structure type with a lower Si/Al ratio than Y) discussed by Lechert et al.[21] It was assumed that the gel phase causes the formation of structural elements such as six-rings that may act as precursors for the nucleation events. This may occur preferably at the gel–liquid interface, where precursor structures can be formed by transport of small species from solution, or by structural reorganization within the surface region (for example, by partial hydrolysis and rearrangement of surface-bound rings).[21]

The next stages observed during the synthesis were after hydrothermal treatment for 38, 48, 55, and 75 h. The TEM images revealed that while increasing the crystallization time from 28 h (Figure 2b) to 48 h (Figure 2c), the amorphous aggregates were consumed and crystalline particles of FAU-type zeolites were obtained. All crystals have the typical octahedral morphology of the FAU-type zeolite. Close examination of the images taken at different crystallization times indicates that all crystals are single, and that the particle size is rather uniform. This implies that only one nucleus was present in each gel particle. To ascertain the representative nature of the HR-TEM samples, different stages of crystallization were examined with DLS. Particles with sizes of 25–35 nm were present in the initial synthesis mixture and in the products obtained after heating up to 28, 38, 48, and 55 h. In situ DLS measurements and TEM results are therefore in good agreement. The data show that as crystallization time increases, the overall size of the zeolite-gel particles remains approximately constant, suggesting that the nutrients for the crystal growth were primarily supplied by the gel particles. This is confirmed by the stable mass balance of the solutions 1) containing the amorphous precursor gel particles two hours after mixing, 2) after two days of aging at RT, and 3) after hydrothermal treatment at 100 °C for 48 h (1.7 ± 0.1 wt% solid content throughout).

The XRD patterns show that all products obtained after 38 h are highly crystalline FAU zeolite (Figure 1d–f). Further evidence for the emerging FAU structure in the early stages of particle growth is provided by IR spectroscopy. The IR spectra of FAU samples after 28 and 55 h contain a band at approximately 570 cm^{-1} in addition to the band at 470 cm^{-1} (Figure 3c, d). The appearance of the band at 570 cm^{-1}, first evident after 28 h, is associated with the FAU structure (this band is not observed for amorphous silica; see Figure 3b).

To probe the association of the organic template with the primary gel aggregates existing in the initial solutions and in the zeolite crystals (heated for 48 h), thermogravimetric analysis (TGA) of washed samples was performed. The TGA data for the gel aggregates show the presence of large quantities of organic template, decomposing at around 236 °C in air (ca. 32 wt% based on calcined gel, after water desorption, Figure 5). The FAU sample also contains the organic TMA template, but it decomposes in two steps at higher temperatures (335 and 487 °C), suggesting different local environments of the template (ca. 10 wt% total, the remainder is adsorbed water).

After keeping the initial mixture at 100 °C for an extended period (75 h), well-defined octahedral crystals with sizes of about 50 nm were formed (Figure 2d). Since no gel particles remained in the solution after 48 h, the nutrients for this extended growth must have been the colloidal zeolites themselves. The important point is that the FAU zeolite crystals can continue to grow through solution transport over macroscopic distances.

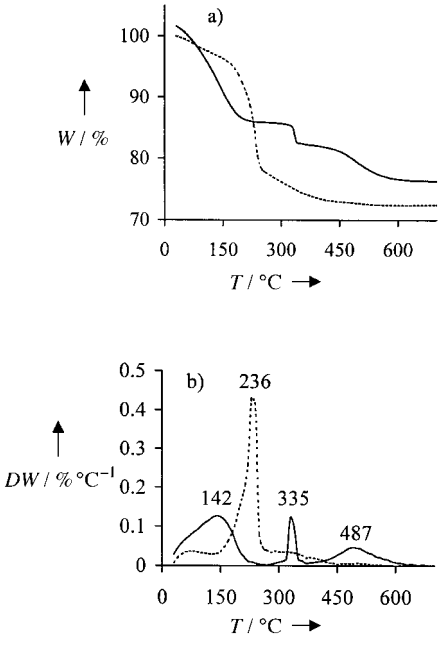

Figure 5. a) Thermogravimetric (TG) and b) derivative TG curves of TMA-containing primary gel aggregates present in the initial solution before heating (dotted line) and of the FAU nanocrystals obtained after 48 h of heating at 100 °C (solid line; heating rate 10 °C min^{-1} in air).

  1433-7851/99/3821-3203 $ 17.50+.50/0

The direct evidence obtained here with high-resolution electron microscopy reveals the mechanism of FAU zeolite nucleation and crystal growth at elevated temperatures (Figure 6). FAU crystals are nucleated in amorphous gel

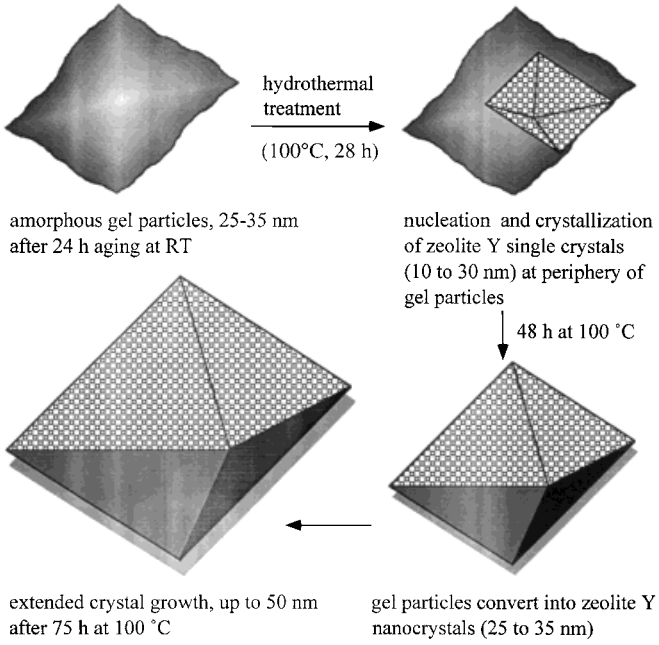

Figure 6. Proposed reaction scheme for the zeolite growth mechanism in colloidal solution.

aggregates existing in the colloidal aqueous solution after 28 h. Each amorphous aggregate nucleates only one single zeolite crystal, with nucleation always beginning at the gel–solution interface. Our results confirm a previously proposed nucleation mechanism for this type of zeolite, where structural elements at the periphery of the gel phase act as precursors for the nucleation events. The aggregates are completely converted into crystalline zeolite Y within 48 h at 100 °C. Solution mass transfer is the dominant mechanism for the substantial crystal growth of FAU crystals after prolonged crystallization times.

Experimental Section

The synthesis of FAU from a clear aqueous solution with a molar composition of 0.15 Na_2O:5.5 $(TMA)_2O$:2.3 Al_2O_3:10 SiO_2:570 H_2O was performed at 100 °C. Tetramethylammonium hydroxide pentahydrate ($TMAOH \cdot 5H_2O$; Aldrich) was added to an aqueous solution of aluminum isopropoxide (Aldrich) to give a clear solution. Then silica sol (30 %, 5 nm, pH 10, Aldrich) was added while stirring, and the mixture was further stirred for about 30 min. Crystallization was carried out in Teflon-lined stainless steel autoclaves at 100 °C. Prior to analysis all samples were purified three times by high-speed centrifugation, removal of the mother liquor, and redispersion in water.

The XRD data were collected on a Scintag XDS 2000 diffractometer using $Cu_{K\alpha}$ radiation. The TG measurements were performed with a 951 DuPont Instruments Analyzer. The samples were examined with a Philips 200 FEG TEM operated at 200 kV. The grid covered with colloidal suspension was dried and scanned at low magnification to search for the crystals. Focusing and astigmatism correction were performed at the working magnification on an area about 2.5 μm from the area of interest to decrease the amount of beam damage to the specimen. The beam was then automatically translated back to the previous area before the image was captured by a Gatan 794 multiscan charge-coupled device camera.

Received: April 30, 1999 [Z13351IE]
German version: *Angew. Chem.* **1999**, *111*, 3405 – 3408

Keywords: colloids · crystal growth · zeolites

[1] R. M. Barrer, *Hydrothermal Chemistry of Zeolites*, Academic Press, London, **1982**.
[2] S. L. Burkett, M. E. Davis in *Solid-State Supermolecular Chemistry: Two- and Three-Dimensional Inorganic Networks, Comprehensive Supermolecular Chemistry, Vol. 7* (Eds.: G. Alberti, T. Bein), Elsevier, Tarrytown, NY, USA, **1996**, pp. 465 – 483.
[3] H. Kessler in *Solid-State Supermolecular Chemistry: Two- and Three-Dimensional Inorganic Networks, Comprehensive Supermolecular Chemistry, Vol. 7* (Eds.: G. Alberti, T. Bein), Elsevier, Tarrytown, NY, USA, **1996**, pp. 425 – 464.
[4] M. E. Davis, R. F. Lobo, *Chem. Mater.* **1992**, *4*, 756 – 768.
[5] a) S. Feng, T. Bein, *Nature* **1994**, *368*, 834 – 836; b) S. Feng, T. Bein, *Science* **1994**, *265*, 1839 – 1841; c) S. Mintova, B. J. Schoeman, V. Valtchev, J. Sterte, S. Mo, T. Bein, *Adv. Mater.* **1997**, *9*, 585 – 589; d) T. Bein, *Chem. Mater.* **1996**, *8*, 1636 – 1653; e) J. Jansen, *Micropor. Mesopor. Mater.* **1998**, *21*, 213 – 226.
[6] S. L. Burkett, M. E. Davis, *Chem. Mater.* **1995**, *7*, 920 – 928.
[7] J. N. Watson, L. E. Iton, R. I. Keir, J. C. Thomas, T. L. Dowling, J. W. White, *J. Phys. Chem. B* **1997**, *101*, 10094 – 10104.
[8] W. Bo, M. Hongzhu, *Micropor. Mesopor. Mater.* **1998**, *25*, 131 – 136.
[9] O. Terasaki, T. Ohsuna, V. Alfredsson, J.-O. Bovin, D. Watanabe, S. W. Carr, M. W. Anderson, *Chem. Mater.* **1993**, *5*, 452 – 458.
[10] W. H. Dokter, H. F. Garderen, T. P. M. Beelen, R. A. Santen, W. Bras, *Angew. Chem.* **1995**, *107*, 122 – 125; *Angew. Chem. Int. Ed. Engl.* **1995**, *34*, 73 – 75.
[11] M. Tsapatsis, M. Lovallo, M. E. Davis, *Micropor. Mater.* **1996**, *5*, 381 – 388.
[12] B. Subotic, *Micropor. Mater.* **1995**, *4*, 239 – 242.
[13] C. S. Cundy, M. S. Henty, R. J. Plaised, *Zeolites* **1995**, *15*, 342 – 352.
[14] S. Ritsch, N. Ohnishi, T. Ohsuna, K. Hiraga, O. Terasaki, Y. Kubota, Y. Sugi, *Chem. Mater.* **1998**, *10*, 3958 – 3965.
[15] P. E. A. Moor, T. P. M. Beelen, R. A. Santen, K. Tsuji, M. E. Davis, *Chem. Mater.* **1999**, *11*, 36 – 43.
[16] R. Gougeon, L. Delmotte, D. L. Nouen, Z. Gabelica, *Micropor. Mesopor. Mater.* **1998**, *26*, 143 – 151.
[17] J. Shi, M. W. Anderson, S. W. Carr, *Chem. Mater.* **1996**, *8*, 369 – 375.
[18] H. Kacirek, H. Lechert, *J. Phys. Chem.* **1976**, *80*, 1291 – 1296.
[19] D. M. Ginter, A. T. Bell, C. J. Radke, *Zeolites* **1992**, *12*, 742 – 749.
[20] H. Lechert, *Zeolites* **1996**, *17*, 473 – 482.
[21] H. Lechert, H. Kacirek, *Zeolites* **1993**, *13*, 192 – 199.
[22] M. W. Anderson, J. R. Agger, J. T. Thornton, N. Forsyth, *Angew. Chem.* **1996**, *108*, 1301 – 1304; *Angew. Chem. Int. Ed. Engl.* **1996**, *35*, 1210 – 1213.
[23] A. E. Persson, B. J. Schoeman, J. Sterte, J.-E. Otterstedt, *Zeolites* **1994**, *14*, 557 – 567.
[24] S. Mintova, S. Mo, T. Bein, *Chem. Mater.* **1998**, *10*, 4030 – 4036.
[25] J. Dougherty, L. E. Iton, J. W. White, *Zeolites* **1995**, *15*, 640 – 649.
[26] L. Gora, K. Streletzki, R. W. Thompson, G. D. J. Phillies, *Zeolites* **1997**, *18*, 119 – 131.
[27] O. Regev, Y. Cohen, E. Kehat, Y. Talmon, *Zeolites* **1994**, *14*, 314 – 319.
[28] S. Mintova, N. Olson, V. Valtchev, T. Bein, *Science* **1999**, *283*, 958 – 960.
[29] M. M. J. Treacy, J. B. Higgins, R. Ballmoos, *Collection of Simulated XRD Powder Patterns for Zeolites*, Elsevier, New York, **1996**.

  1433-7851/99/3821-3204 $ 17.50+.50/0